Effect of Lipid Composition on the Structure and Theoretical Phase Diagrams of DC-Chol/DOPE-DNA Lipoplexes

ARTICLE *in* BIOMACROMOLECULES · NOVEMBER 2010

Impact Factor: 5.75 · DOI: 10.1021/bm1008124 · Source: PubMed

6 AUTHORS, INCLUDING:

Mónica Muñoz Ubeda
Materials Science Institute of Barcelona
12 PUBLICATIONS **200** CITATIONS
SEE PROFILE

Alberto Rodriguez-Pulido
Madrid Institute for Advanced Studies
17 PUBLICATIONS **245** CITATIONS
SEE PROFILE

Aurora Nogales
Spanish National Research Council
137 PUBLICATIONS **2,419** CITATIONS
SEE PROFILE

Alberto Martin-Molina
University of Granada
52 PUBLICATIONS **944** CITATIONS
SEE PROFILE

Effect of Lipid Composition on the Structure and Theoretical Phase Diagrams of DC-Chol/DOPE-DNA Lipoplexes

Mónica Muñoz-Úbeda,[†] Alberto Rodríguez-Pulido,[‡] Aurora Nogales,[§] Alberto Martín-Molina,[||] Emilio Aicart,[†] and Elena Junquera*[,†]

Grupo de Química Coloidal y Supramolecular, Departamento de Química Física I, Facultad de Ciencias Químicas, Universidad Complutense de Madrid, 28040 Madrid, Spain, Department of Polymer Chemistry, Zernike Institute for Advanced Materials, University of Groningen, Nijenborgh 4, Groningen, 9747 AG Netherlands, Instituto de Estructura de la Materia, CSIC, Serrano 121, 28006 Madrid, Spain, and Grupo de Física de Fluidos y Biocoloides, Departamento de Física Aplicada, Facultad de Ciencias, Universidad de Granada, 18071-Granada, Spain

Received July 19, 2010; Revised Manuscript Received October 8, 2010

Lipoplexes constituted by calf-thymus DNA (CT-DNA) and mixed cationic liposomes consisting of varying proportions of the cationic lipid 3β-[*N*-(*N*′,*N*′-dimethylaminoethane)-carbamoyl]cholesterol hydrochloride (DC-Chol) and the zwitterionic lipid, 1,2-dioleoyl-*sn*-glycero-3-phosphoetanolamine (DOPE) have been analyzed by means of electrophoretic mobility, SAXS, and fluorescence anisotropy experiments, as well as by theoretically calculated phase diagrams. Both experimental and theoretical studies have been run at several liposome and lipoplex compositions, defined in terms of cationic lipid molar fraction, α, and either the mass or charge ratios of the lipoplex, respectively. The experimental electrochemical results indicate that DC-Chol/DOPE liposomes, with a mean hydrodynamic diameter of around (120 $\pm$ 10) nm, compact and condense DNA fragments at their cationic surfaces by means of a strong entropically driven electrostatic interaction. Furthermore, the positive charges of cationic liposomes are compensated by the negative charges of DNA phosphate groups at the isoneutrality *L*/*D* ratio, $(L/D)_\phi$, which decreases with the cationic lipid content of the mixed liposome, for a given DNA concentration. This inversion of sign process has been also studied by means of the phase diagrams calculated with the theoretical model, which confirms all the experimental results. SAXS diffractograms, run at several lipoplex compositions, reveal that, irrespectively of the lipoplex charge ratio, DC-Chol/DOPE-DNA lipoplexes show a lamellar structure, L_α, when the cationic lipid content on the mixed liposomes $\alpha \geq 0.4$, while for a lower content ($\alpha = 0.2$) the lipoplexes show an inverted hexagonal structure, H_{II}, usually related with improved cell transfection efficiency. A similar conclusion is reached from fluorescence anisotropy results, which indicate that the fluidity on liposome and lipoplexes membrane, also related with better transfection results, increases as long as the cationic lipid content decreases.

Introduction

Nowadays, lipoplexes (cationic lipids + DNA) are an increasing area of research because mixed liposomes, formed by cationic and zwitterionic helper lipids, are revealing as the most promising nonviral vectors in gene therapy.[1−8] It is well-known that the efficiency of DNA transfection using cationic lipids is improved by the presence of a neutral helper lipid[4,6,9] and it is highly dependent on the kind of the cationic and the helper lipid, the mixed lipid composition, and the lipid/DNA ratio.[4,6,9] However, a universal behavior can be reached for the lamellar phase when the transfection efficiency is compared with respect to charge density of the mixed liposomes.[10,11] From those previous studies, it is clear that the electrostatic interaction between cationic liposomes and anionic DNA plays an important role in the lipoplex properties, which reinforces the interest on improving the knowledge of this interaction from both experiments and theory.[6,9] In this sense, a physicochemical study of the DNA compaction by cationic lipids should shed light, not only on the formation process of lipoplexes, but also on the transfection mechanisms.

Scheme 1. (a) Cationic Lipid Molecule, DC-Chol, and (b) Zwitterionic Lipid Molecule, DOPE

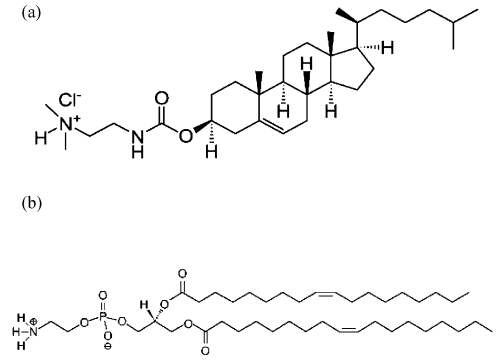

Lipoplexes formed by a cationic lipid derived from cholesterol (DC-Chol, see Scheme 1) and a zwitterionic helper lipid of the phosphatidylethanolamine family (DOPE, see Scheme 1) have been studied elsewhere not only from a biological standpoint,[12−21] but also from a physicochemical point of view.[22−28] In fact, DOPE is frequently used in transfection because it increases

* To whom correspondence should be addressed. Tel.: +34-913944131. Fax: +34-913944135. E-mail: junquera@quim.ucm.es. http://www.ucm.es/info/coloidal/index.html.
[†] Universidad Complutense de Madrid.
[‡] University of Groningen.
[§] Instituto de Estructura de la Materia.
[||] Universidad de Granada.

10.1021/bm1008124
Published on Web 11/08/2010

the elasticity of liposome bilayer and promotes the fusion of lipoplexes with the cell membrane, which results in an increase of the DNA transfection efficiency.[4,11,22,29−35] In addition, we reported recently[28] an experimental study of DNA compaction with the mixed liposome DC-Chol/DOPE at equimolar lipid composition. However, the charge density at the surface and the composition of the mixed liposome, as well as their structural characteristics, seem to be key factors on the properties of the resulting lipoplexes, and, accordingly, on their potential efficiency as cell transfectors.[5,11] In fact, cationic lipoplexes may form lamellar, hexagonal, or even cubic structures, that interact with the cell membranes in a very different way and with a different effectiveness; it has been reported that hexagonal phases promote better transfection yields.[5,11] Thus, it results of relevance to conjugate the capacity of liposomes to condense and compact DNA by forming strong and stable lipoplexes, with a relative ease to release DNA into the cells. Therefore, given that factors such as the lipid composition and the charge ratio of the lipoplex seem to be of great importance, in the present work we report a more extensive study of this lipoplex covering the whole range of the mixed lipid composition and at several lipid/DNA charge ratios. Thus, the objective and the main contribution of this work are to experimentally analyze in depth and to predict, from a theoretical standpoint, the influence of these factors on the compaction process and on the behavior of the DC-Chol/DOPE-DNA lipoplexes.

To carry on this study, the lipoplexes have been characterized by means of several experiments. Electrochemical methods, such as zeta potential, are a powerful tool to analyze the electrostatic interactions on the surface of the liposomes and the lipoplexes.[4,34,36−40] Fluorescence anisotropy is used to check the fluidity of the lipidic bilayer of liposomes in the absence and presence of DNA, which is related to the release of DNA into the mammalians cells.[34,39,41−51] In addition and with the object of determining the structure of the lipoplexes, this work also reports experiments of small-angle X-ray scattering (SAXS) run at different lipid composition and charge ratios. Furthermore, the compaction process of DNA by the cationic liposomes has also been theoretically analyzed by using a theory recently developed for the interaction among liposomes and polyelectrolytes.[52,53] Phase diagrams of the resulting lipoplexes, built at the experimentally studied mixed lipid compositions, include the charge inversion and re-entrant condensation processes among the lipoplexes. These phase diagrams contain interesting information to have either anionic or cationic isolated lipoplexes or also clusters of lipoplexes. In particular, it may provide a route to predict the optimal concentrations of DNA and mixed liposome so as to obtain stable complexes in electrolytic solutions from a physicochemical stand point. Nevertheless, this does not mean that such theoretical predictions are sufficient to improve on their own the transfection process, because it leaves out many effects that should be taken into account once the lipoplexes are inside the cell. Accordingly, the combination of the model and the experimental characterization performed in this work provides a first step toward an improved understanding of these complex systems.

Experimental Details

Materials. Cationic lipid, 3β-[*N*-(*N*′,*N*′-dimethylaminoethane)-carbamoyl]cholesterol hydrochloride (DC-Chol), and zwitterionic lipid 1,2-dioleoyl-*sn*-glycero-3-phosphoetanolamine (DOPE) were from Avanti Polar Lipids. Cationic lipid belongs to the sterols family and DOPE contains an unsaturation on the *cis* configuration at the 9 position of both hydrocarbon chains (see Scheme 1). Sodium salt of calf thymus DNA (CT-DNA) was from Sigma-Aldrich. All of them, with the best purities, were used without further purification. Solutions were prepared with distilled and deionized water (Super Q Millipore system, conductivity lower than 18 μS cm^{-1}), and all were buffered with PBS buffer at around physiological conditions (pH = 7.5 and ionic strength of 160 mM).

Preparation of Solutions. Liposome and lipoplex solutions were prepared according to a protocol widely explained elsewhere.[54] Several lipid compositions (in terms of molar fractions, α, and lipoplex compositions (in terms of either mass ratio, *L*/*D*, or charge ratio, CR) were prepared. These quantities are defined as follows:

$$\alpha = \frac{n_{L^+}}{n_{L^+} + n_{L^0}} \tag{1}$$

$$\frac{L}{D} = \frac{L^+ + L^0}{D} \tag{2}$$

$$\mathrm{CR} = \frac{n^+}{n^-} = \frac{L^+/M_{L^+}}{2D/\bar{M}_{\mathrm{bp}}} \tag{3}$$

where n_{L^+} and n_{L^0} stand for the number of moles of cationic and zwitterionic lipids, respectively; n^+ and n^- are the number of moles of positive and negative charges, coming from cationic lipid and DNA, respectively; L^+ and L^0 are the masses of cationic and zwitterionic lipids (thus, $L = L^+ + L^0$, is the total mass of lipid); M_{L^+} is the molar mass of cationic lipid and $\bar{M}_{\mathrm{bp}}$ is the average molar mass per DNA base pair. A stock solution of CT-DNA was prepared two days before the mixing with liposomes. DNA concentrations (expressed in mM base pairs) were determined by absorbance at 260 nm (ε = 6600 M^{-1} cm).[55,56] A A_{260}/A_{280} ratio of 1.90 and a negligible absorbance at 320 nm ($A_{320} = -0.003$) reveal[35,55−57] that the contamination of the DNA used in this work by the presence of a certain percentage of proteins is negligible.

Experimental Methods. The phase Analysis Light Scattering technique (*Zeta PALS*, Brookhaven Instrum. Corp., U.S.A.) was used to measure electrophoretic mobilities (and from it, zeta potential) and particle sizes. This interferometric technique is up to 1000 times more sensitive than traditional light scattering methods based on the shifted frequency spectrum and uses phase analysis light scattering to determine the electrophoretic mobility of charged colloidal suspensions. Temperature was controlled at (298.15 ± 0.01 K). Each electrophoretic mobility data is taken as an average of over 50 independent measurements. Electrophoretic mobility for liposome and lipoplex solutions was measured at each α as a function of *L*/*D* ratio.

Small-angle X-ray scattering (SAXS) experiments were carried out on a Bruker AXS nanostar small-angle X-ray scattering instrument. The instrument uses Cu KR radiation (1.54 Å) produced in a sealed tube. Samples were placed in sealed glass capillaries purchased from Hilgenberg with an outside diameter of 1.5 mm and wall thickness of 0.01 mm. The sample chamber is under vacuum. The scattered X-ray are detected on a two-dimensional multiwire area detector (Bruker Hi-Star) and can be converted to one-dimensional scattering by radial averaging and represented as a function of momentum transfer vector q ($= 4\pi \sin\theta/\lambda$) in which θ is half the scattering angle and λ is the wavelength of the incident X-ray beam. The sample to detector distance was 0.63 m. Measurements on each sample were collected over four cycles of 30 min each to ensure the stability of the lipoplexes. SAXS experiments were run at three different CR ratios in the whole range of composition.

Fluorescence anisotropy of diphenylhexatriene (DPH) probe was measured with a Perkin-Elmer LS-50B Luminiscence Spectrometer by following an experimental protocol widely explained elsewhere.[58] Anisotropy values r ($= (I_{VV} - GI_{VH})/(I_{VV} + 2GI_{VH})$) were determined by measuring the intensities of the light emitted by DPH probe, with

the excitation and the emission polarized following the modes vertical−vertical, I_{VV}, vertical−horizontal, I_{VH}, horizontal−horizontal, I_{HH}, and horizontal−vertical, I_{HV}. The instrument grating factor, G (= I_{HV}/I_{HH}), estimated as an average of 10 measurements for each solution, allows to correct optical and electronic differences in the parallel and perpendicular channels. The influence of the light scattering of samples in anisotropy values was also evaluated and considered with the corresponding blank solutions. Each anisotropy value is an average over 36 experimental independent measurements.

Theoretical Background. As in a previous work,[59] the formalism derived by Sennato et al.[52] has been used to analyze theoretically the complexation of liposomes and DNA. This formalism is in turn based on the theory developed by Nguyen and Shklovskii[60,61] to describe the complexation of a long flexible charged polyelectrolyte with oppositely charged spherical and rod-like particles. According to the model, a phase diagram can be obtained to characterize the whole complexation process in which lipoplexes experience aggregation (condensation) and disaggregation (reentrant condensation) as a function of the liposome−DNA ratio. Namely, for a given concentration of DNA and growing concentration of liposomes, lipoplexes experience aggregation at some critical concentration, S_a, below isoneutrality, and remain in this aggregated (or condensed) state up to another concentration, S_d, above isoneutrality. For concentrations of liposomes higher than S_d, clusters of lipoplexes start to disaggregate as a consequence of a charge inversion process.[52,59] Although the molecular origin of this last counterintuitive process is not explained in detail by the model, it is qualitatively justified in terms of the correlation-induced attraction of a new liposome to a neutral complex at the isoelectric point. For these liposome concentrations, a new liposome could push away liposomes from the complex, unwind some of the DNA from them, and wind it on itself.[52,59] Anyhow, according to Sennato et al., a more realistic model is required to include factors such as the rigidity of the DNA that undoubtedly would play a relevant role in the reentrant aggregation.[52,59]

In summary, this phenomenological theory predicts that for a given concentration of DNA, P, the system can be described in terms of the DNA concentration in the limit of negligible liposome concentrations, P_0, that is, DNA concentration in equilibrium with lipoplexes. The resulting phase diagram is given by two equations that can be solved in terms of P_0 and E_0 parameters, last one related to the energy gained per complex normalized by the number of DNA polyions, N_i, necessary to neutralize the liposome charge ($N_i = Q/w$).

$$S_a \frac{Q}{w}\left(1 + \sqrt{\frac{2C|E_0|}{wQ}}\right) = P - P_0 \exp\left(\sqrt{\frac{2wQ|E_0|}{C(k_BT)^2}}\right) \quad (4)$$

$$S_d \frac{Q}{w}\left(1 - \sqrt{\frac{2C|E_0|}{wQ}}\right) = P - P_0 \exp\left(-\sqrt{\frac{2wQ|E_0|}{C(k_BT)^2}}\right) \quad (5)$$

where $-w$ and l are the total charge and contour length of DNA, respectively; Q is the positive charge of liposomes and $C = 4\pi\varepsilon_0\varepsilon R$ is the electrical capacitance, ε_0 and ε being the vacuum and relative permittivity, respectively, and R the liposome radius). This set of equations allows us to calculate the two boundaries concentration of liposomes S_a and S_d. The concentration of liposomes where the aggregates are neutrally charged (isoneutrality) can be obtained as well from the model. This liposome concentration, denoted as S_ϕ, is given by[52,61]

$$S_\phi = \frac{P - P_0}{N_i} \quad (6)$$

This concentration can be also expressed in terms of theoretical isoneutrality mass ratio, $(L/D)_{\phi,theo}$, by means of

$$(L/D)_{\phi,theo} = \frac{S_\phi(P)\Phi}{P\bar{\Lambda}}\left(\frac{\alpha M_{L^+} + (1-\alpha)M_{L^0}}{M_{bp}}\right) \quad (7)$$

where $\bar{\Lambda}$ is the average number of base pairs per DNA segment and Φ is the number of lipids per liposome.

Results and Discussion

It is known that many properties of lipoplexes change at the so-called isoneutrality point, that, in terms of lipoplex composition, is defined as the L/D ratio, $(L/D)_\phi$, at which the negative charges of DNA are neutralized by the positive charges of the liposomes, or, in other words, the composition at which the charge ratio of the lipoplexes, CR, equals 1 in eq 3. Furthermore, this parameter defines the lower limit of the lipoplex composition range from which the net charge of the complex is positive, a necessary requirement for transfecting the cells. Several experimental methods have been used to determine this ratio, but the most direct way of doing so is to work with electrochemical properties, such as, electrophoretic mobility, μ_E, zeta potential, ζ, or the surface charge density enclosed by the shear plane, σ_ζ, because all of them show an inversion of sign at this particular L/D value. In this work, ζ values have been obtained from electrophoretic mobility, using Henry equation with Smoluchowski limit.[62] Characteristic sigmoidal curves are usually obtained when representing μ_e, or ζ as a function of either L/D ratio or CR (see the inset of Figure 1, as an example, for the system studied in this work at $\alpha = 0.25$). In these graphs one can observe how lipoplexes show net negative or positive μ_e or ζ values below or above, respectively, a particular L/D ratio assigned to the isoneutrality, $(L/D)_\phi$. This inversion of sign reveals that the electrostatical interaction among liposomes and DNA takes place at the surface of the colloidal aggregates, the release of chloride and sodium counterions from cationic lipid and DNA phosphates, respectively, being the driving force. From these electrophoretic data, we obtain directly the experimental values of S_a, S_ϕ, and S_d, being those liposome concentrations at which the mobility stars to decrease, reaches the isoneutrality and achieve a maximum, respectively. As it will be shown later, these values will be used as input parameters to build the corresponding theoretical phase diagrams. Figure 1 shows the effect that mixed liposome composition, α, has on this isoneutrality ratio. As expected, as long as the content of cationic lipid increases on liposome composition, the isoneutrality is reached at lower L/D ratios, for a given DNA concentration. PALS technique also allows for the determination of the sizes of mixed liposomes; an average hydrodynamic diameter of (120 ± 10) nm has been obtained in agreement with cryo-TEM results, previously reported by us for this lipoplex at $\alpha = 0.5$.[28] No other effect of lipid composition was observed due to the fact that DC-Chol and DOPE lipids, although with different shape, have a hydrophobic region with a similar length (see Scheme 1).

This inversion of sign process has been also analyzed, from a theoretical point of view, by means of the aggregation−disaggregation theoretical model (or condensation/re-entrant condensation), briefly presented in a previous section. This model has been applied to predict the phase diagrams of the lipoplexes studied in this work, consisting of plots of DNA concentration, P, versus liposome concentration, S, with the characteristic boundary lines for aggregation, $S_a(P)$, and disaggregation, $S_d(P)$, as well as the electroneutrality lines, $S_\phi(P)$, at which the lipoplex charge inverts the sign. Table 1 displays the input data required to calculate the free parameters P_0 and E_0 of the theory by

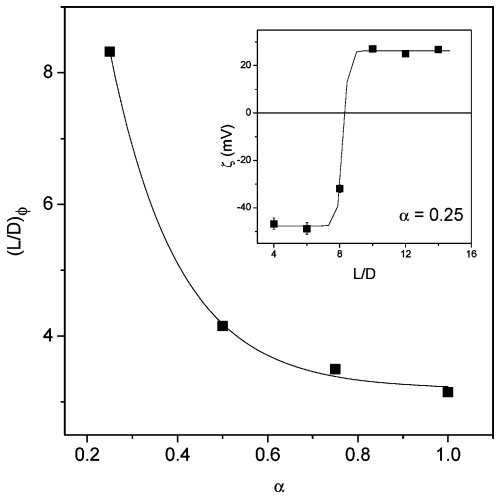

Figure 1. Electrochemical study: the main figure shows the values of isoneutrality L/D ratios, $(L/D)_\phi$, as a function of mixed liposome composition in terms of molar fractions, α. Inset: Plot of zeta potential, ζ, as a function of lipoplex composition L/D, for lipoplexes with α = 0.25 in aqueous buffered medium at 298.15 K. Solid line: sigmoidal fit of experimental values. Errors are estimated to be around 3%. DNA concentration was kept constant at 0.05 mg/mL and the total lipid concentration was varied, depending on the lipid composition, to cover a wide L/D ratio range (in the inset from 4 to 14).

Table 1. Input Parameters on the Aggregation−Disaggregation Theory and Results Obtained for DC-Chol/DOPE-DNA Lipoplexes at Three Different Liposome Compositions, α

parameter[a]	α = 0.25	α = 0.5	α = 1
R/nm	49.5	49.5	49.5
10^{16} C/(C^2 J^{-1})	4.323	4.323	4.323
Φ/(lipids/liposome)	87000	88400	92800
Q/(C/e)	12000	24450	51300
w/(C/e)	5400	5400	5400
10^{-15} P/(DNA segments/L)	17.16	17.16	17.16
10^{-15} $S_a(P)$/(liposomes/L)	3.90	1.83	1.33
10^{-15} $S_d(P)$/(liposomes/L)	4.30	2.49	2.11
10^{29} E_0/(J)	0.67	4.57	24.81
10^8 E_0/kT	0.16	1.11	6.03
10^{-15} P_0/(DNA segments/L)	8.04	7.21	3.64
10^{-15} $S_\phi(P)$/(liposomes/L)	4.11	2.20	1.42

[a] R, liposome radius (errors of ±0.5 nm); C, liposome capacitance; Φ, number of lipids per liposome; Q, liposome charge; w, charge of DNA segment; P, DNA concentration; $S_a(P)$, liposome concentration at aggregation; $S_d(P)$, liposome concentration at disaggregation; E_0, DNA−liposome interaction energy; P_0, DNA concentration in equilibrium with lipoplexes; and $S_\phi(P)$, liposome concentration at isoneutrality.

solving eqs 4 and 5, as well as the obtained results. In particular, P is the DNA concentration used in the electrophoretic experiments, w is based on the 2700 bp fragments on average obtained from agarose gel electrophoresis experiments, Q is calculated from the surface area of the liposome and the estimated area for the headgroup of the lipid, E_0 and P_0 are phenomenological parameters related to the strength of liposome−DNA binding and DNA concentration in equilibrium with the lipoplexes, respectively, and the values of $S_a(P)$ and $S_d(P)$ are obtained from electrophoresis experiments. Several remarks can be extracted from results in Table 1: (i) it can be noticed that $P_0 \ll P$ in all cases, which agrees with the assumption consisting in that most of the DNA molecules are forming complexes; (ii) accordingly, the total energy required for DNA complexation (normalized by the thermal energy, k_BT) is much lower than 1, in agreement with the spontaneous condensation of DNA by liposomes observed in the experiments; (iii) it is also remarkable that a higher E_0 is predicted by the theory when the proportion of zwitterionic lipid increases, which agrees with the fact that the

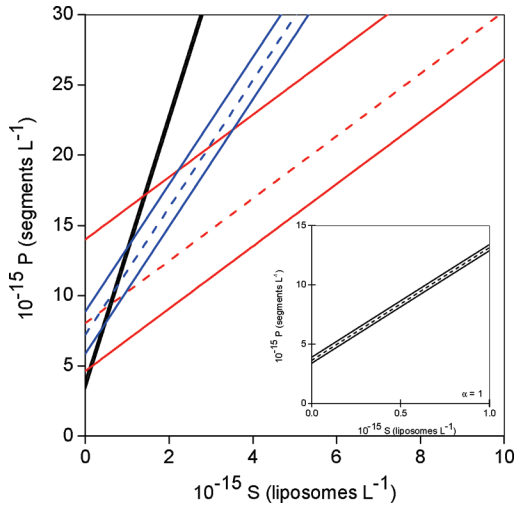

Figure 2. Phase diagram for DC-Chol/DOPE-DNA lipoplexes with a liposome composition of α = 0.25 (red), 0.5 (blue), and 1 (black), according to the aggregation−disaggregation theory. Solid lines are $S_a(P)$ and $S_d(P)$, while dashed line is $S_\phi(P)$. Inset: Zoom view of the phase diagram at α = 1.

interaction energy between the DNA and cationic lipids is more intense than that between the polyanion and the zwitterionic lipids. Even so, the theory predicts very small E_0 values for the three compositions, which could be indicating that a change on liposome composition does not affect appreciably the interaction energy between DNA and liposomes. Finally, these values for E_0 and P_0 are of the same order of magnitude as those reported for similarly charged lipoplexes made of DODAB/DOPE-DNA and DODAB/DLPC-DNA.[59]

Figure 2 shows the theoretical phase diagram for DC-Chol/DOPE-DNA lipoplexes at the three liposome compositions. Given a constant value for E_0 and P_0, the phase diagram predicts the existence of negatively charged stable lipoplexes at $S < S_a(P)$ in excess of free anionic polyelectrolite. If S increases, lipoplexes may experience aggregation and clusters of lipoplexes are formed. Previously reported cryo-TEM micrographs[28,54,59] for other lipoplexes and for that one studied in this work with α = 0.5, confirm the formation of these cluster structures. In this domain of S concentration, that is, for $S_a(P) < S(P) < S_d(P)$, the isoneutrality of the lipoplexes, $S_\phi(P)$, is reached and, accordingly, the electrophoretic mobility and, thus, zeta potential is null. However, the theory predicts at this point that complexes attract more cationic liposomes than those required to neutralize the negative charge,[60,61] thus provoking a charge inversion for $S > S_\phi(P)$. Finally, for $S > S_d(P)$, clusters start to partially dissolve, giving rise to stable and free positively charged lipoplexes, in coexistence with the remaining clusters. Scheme 2 shows an illustration of the above-mentioned transitions. It can also be observed in Figure 2 that for a given DNA concentration (draw an imaginary horizontal line) the boundary lines are shifted toward lower liposome concentrations in the order (α = 1) > (α = 0.5) > (α = 0.25), as expected. This feature is in agreement with the fact that the bare charge of liposomes with α = 0.25 is smaller than those ones for α = 0.5 and α = 1. Accordingly, those lipoplexes consisting of liposomes with the cationic lipid as the major component require a lower number of liposomes to induce charge inversion. As a consequence, alterations in the charge of the liposome determine the manner in which the different phase transitions occur. Furthermore, this also involves that the $S_a(P) - S_d(P)$ concentration range gets wider as long as liposome composition, α, decreases. In fact, the three boundary lines (S_a, S_ϕ, and S_d) seem

Scheme 2. Illustrative Diagram of the Transitions Predicted by the Theoretical Aggregation−Disaggregation Model[a]

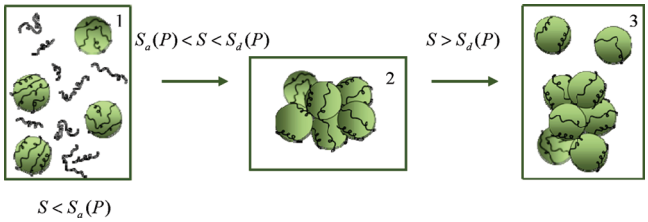

[a] (1) Isolated lipoplexes with net negative charge, in coexistence with the anionic polyelectrolyte DNA; (2) clusters of lipoplexes with net charge around or equal to zero (isoneutrality); and (3) clusters of lipoplexes in coexistence with isolated lipoplexes with net positive charge.

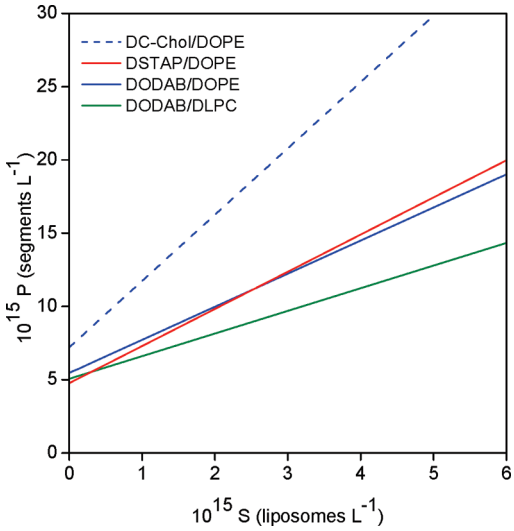

Figure 3. Isoneutrality boundary lines, $S_\phi(P)$, for DC-Chol/DOPE-DNA (this work, blue dashed line), DODAB/DOPE-DNA (solid blue line), DSTAP/DOPE-DNA (red solid line), and DODAB/DLPC-DNA (green solid line) lipoplexes with equimolar lipid compositions, $\alpha = 0.5$.[54]

to coincide for the system with $\alpha = 1$ in the main plot of Figure 2; these lines can be differentiated only in the zoom view of the inset. It means that the liposome concentration range within which lipoplexes aggregate to form clusters and the isoneutrality of the system is reached, gets narrower as long as the content on helper lipid decreases on the mixed liposome, and its positive charge increases. Equation 7 has been used to calculate theoretical isoneutrality mass ratios, $(L/D)_{\phi,\text{theo}}$. For that purpose, Φ has been calculated assuming a lipidic bilayer with a thickness of 4.0 nm, liposome surface areas of the spherical liposomes calculated by using the diameters found in electrophoretic experiments, and polar headgroups with average surfaces, calculated considering the values of the pure lipids and liposome composition, α. Values of 8.1 at $\alpha = 0.25$, 4.1 at $\alpha = 0.5$, and 2.4 at $\alpha = 1$ were obtained, in good concordance with the experimental results.

Figure 3 shows the isoneutrality boundary lines for the lipoplex studied in this work, together with those ones for other lipoplexes studied by us previously,[59] with a mixed liposome composition of $\alpha = 0.5$, for comparison. It is noticeable that for a given DNA concentration the boundary lines are shifted toward higher liposome concentrations in the order DC-Chol/DOPE-DNA < DODAB/DOPE-DNA < DSTAP/DOPE-DNA < DODAB/DLPC-DNA, indicating that those lipoplexes consisting of DOPE as a helper lipid require a lower number of liposomes to induce charge inversion, feature that may be quite advantageous since they may be less cytotoxic. This feature is in agreement with the fact that the bare charge of DODAB/

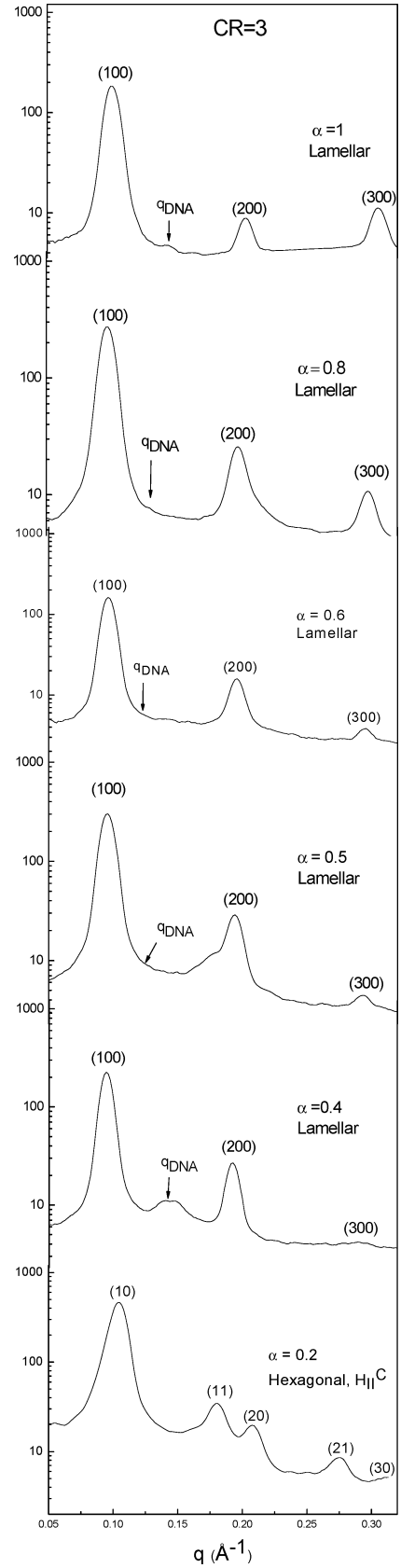

Figure 4. Diffractograms of DC-Chol/DOPE-DNA lipoplexes at different mixed lipid composition, α, and a charge ratio CR = 3. DNA concentration was varied from 0.6 to 2.0 mg/mL and the total lipid concentration was varied from 5 to 32.

DLPC is smaller than those estimated for DC-Chol/DOPE, DODAB/DOPE, and DSTAP/DOPE (see Table 1 on this work

Scheme 3. (a) Lamellar Structure, L_α, and (b) Inverted Hexagonal Structure, H_{II}

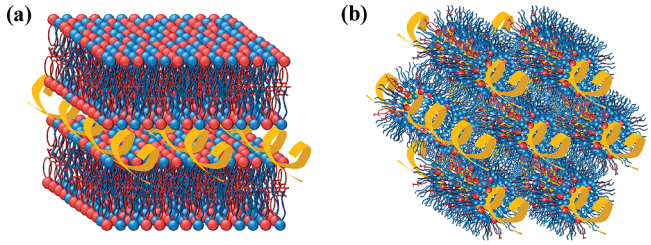

and Table 3 in ref 59) This work corroborates that DOPE is a very appropriate helper lipid, not only from the biochemical experiments on transfecting cells (the efficiency of DOPE as a fusogenic lipid and as a gene transfer agent is widely documented on the literature related with gene therapy),[8,22,33−35,63,64] but also from a physicochemical point of view. In addition, regarding the cationic lipid, it seems that DC-Chol, the cholesterol derivative used in this work, may play a better role on lipofection than its counterparts of dialkylamines (DODAB) or diols (DSTAP) families.

SAXS experiments were carried on covering the whole composition range of the lipid composition, α, at three charge ratios, CR (= 3, 5, and 7), which means that all the lipoplexes are positively charged. Figure 4 shows, as an example, a set of SAXS diffractograms of the lipoplexes, where intensity is plotted versus q factor at CR = 3, for six lipid compositions. Bragg peaks on these diffractograms show that, for $\alpha \geq 0.4$, lipoplexes form a lamellar structure, L_α, with the interlayer distance, d, directly related to the q factor ($d = 2\pi/q_{100}$). Based on that and according to Scheme 3a, lipoplexes can be represented as alternating layers of mixed lipids and DNA helixes where d is the sum of the thicknesses of the lipid bilayer, d_m, and the DNA aqueous layer, d_w. Accordingly, the Bragg peak on the diffractograms not corresponding to the lamellar structure arise from the DNA−DNA correlation, and its q_{DNA} factor permits to obtain the separation between DNA strands in the monolayer, d_{DNA} ($= 2\pi/q_{DNA}$; see Scheme 3a). In those cases where peaks are difficult to see, a protocol consisting of applying a second derivative to the diffractogram in the region where the peak is expected is applied. SAXS results are in good agreement with previously reported cryo-TEM micrographs that confirm the presence of free lipoplexes as well as clusters of lipoplexes with multilamellar structure for DC-Chol/DOPE-DNA lipoplexes with $\alpha = 0.5$ around and above the isoneutrality.[28] Similar conclusions were also extracted for other lipoplexes.[54,59]

Plots of the periodic distance of the lamellar structure, d, versus α and L/D, at the three charge ratios, CR, reported in Figure 5, indicate that d remains roughly constant within an average value of (6.8 ± 0.2) nm. The independency of d versus L/D at constant CR has also been found for other lipoplexes.[65] This feature is due to the fact that DC-Chol and DOPE lipids have a hydrophobic region with a similar length, which implies that the thickness of the mixed lipid bilayer, d_m, should not change with the lipid composition. If a value of $d_m \approx 4.0$ nm is assumed, the thickness of the DNA monolayer, d_w ($= d - d_m$) can be obtained. The calculated value $d_w = (2.8 \pm 0.2)$ nm, obviously independent of α, L/D, and CR, is very consistent with the presence of a monolayer of the hydrated DNA helixes. The results for d and d_m for the lamellar structure are consistent with those ones previously obtained by us with cryo-TEM for either this system at $\alpha = 0.5$[28] or other cationic/zwitterionic lipid−DNA lipoplexes.[59] Furthermore, Figure 6 shows how the separation between the DNA helixes, d_{DNA}, in the aqueous

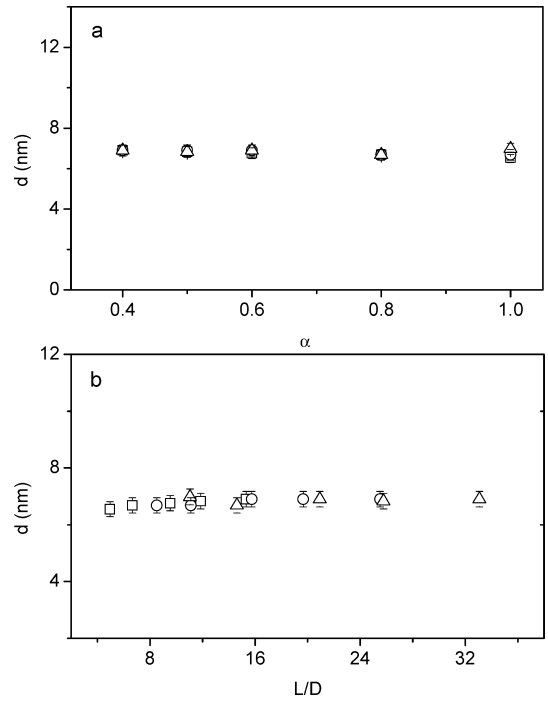

Figure 5. Plots of the periodic distance of the lamellar structure, d, as a function of (a) α and (b) L/D, at charge ratios, CR, of 3 (squares), 5 (circles), and 7 (triangles).

monolayer of the lamellar structure remains approximately constant with α and L/D at the three charge ratios within an average value of (5.2 ± 0.2) nm. Two different behaviors of d_{DNA} versus L/D (at constant CR) have been found in the literature for lipoplexes formed by DNA and DOTAP/DOPE mixed lipids:[65] (i) one for lipoplexes with $L/D < 5$, where d_{DNA} increases with L/D and (ii) another one for lipoplexes with $L/D > 5$, where d_{DNA} remains constant with L/D. This second behavior is in agreement with that one found in Figure 6, due to the fact that d_{DNA} values reported herein have been obtained at L/D ranging from 5 to 34. However, Figure 6 also shows that d_{DNA} remains constant as well with CR, something that initially was unexpected. In fact, by simple geometrical considerations one should expect that at constant CR, d_{DNA} should decreases with α, as it was reported in the literature for DOTAP/DOPE-DNA lipoplexes in water solution.[66] Nevertheless, the same work,[66] from the study reported at high salt concentration (similar to the cell culture solutions and also very similar to that one supplied by the buffer solution used in the present work), concludes that d_{DNA} values at high CR (as we studied here) remains roughly constant with the mixed liposome composition, α. Thus, these authors[66] conclude that both the high ionic strength of the media and the fact that free liposomes and lipoplexes are expected to coexist at high lipid concentrations may be the factors under this trend. This behavior, clearly found as well in Figure 6c, where d_{DNA} is plotted as a function of CR for a given L/D ratio, is very important for transfection of lipoplexes because the high ionic strength of physiological media in cell and tissues affect the efficiency as transfection agents.[66]

On the other hand, the Bragg peaks observed on SAXS diffractogram at $\alpha = 0.2$ of Figure 4 index very well on a $2D$ hexagonal lattice, H_{II}, similar to that one shown in Scheme 3b. The spacing, a, of the cell unit can also be directly related to the q factor ($a = d_{DNA} = 4\pi/(3^{(1/2)}q_{10})$. In this hexagonal lattice, a monolayer of mixed lipids with the zwitterionic DOPE as the major component, surrounds the DNA helixes, the structure of the DNA-mixed lipids resembling inverted cylindrical micelles.

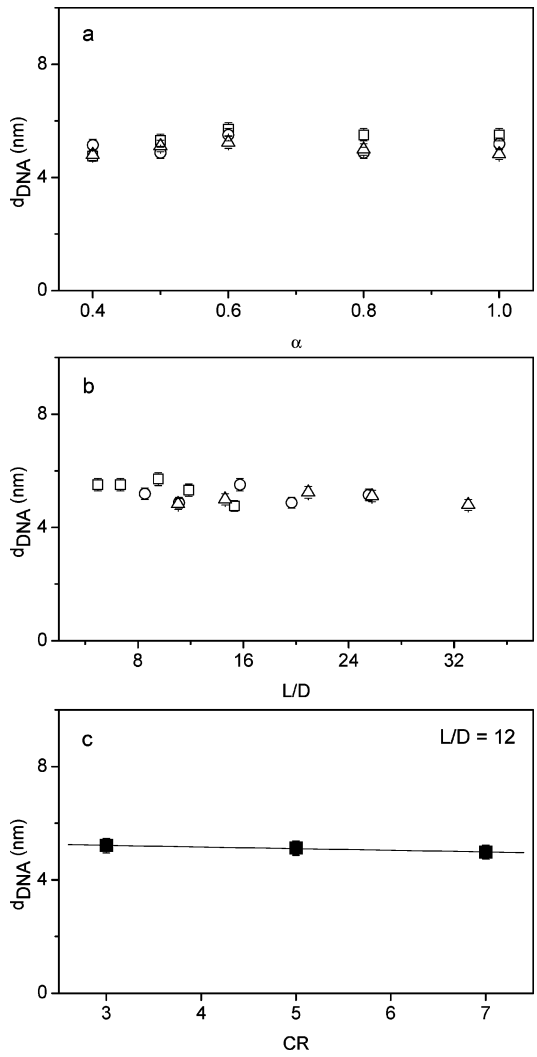

Figure 6. Plots of the distance between DNA helixes on the lamellar structure, d_{DNA}, as a function of (a) α and (b) *L*/*D*, at charge ratios, CR, of 3 (squares), 5 (circles), and 7 (triangles). (c) Plot of d_{DNA} as a function of charge ratio, CR, for $L/D = 12$.

An almost constant value of (6.7 ± 0.2) nm has been obtained on average for $a = d_{DNA}$ at CR = 3, 5, and 7. These values indicate that, in the hexagonal structure with low cationic lipid content, DNA helixes are more separated than in the lamellar one. In any case, and taking into account the lipid chain lengths, the diameter inside the inverted micelle cylinder (equivalent to d_w in the lamellar structure) is (2.7 ± 0.2) nm, which is also consistent with the presence of the hydrated DNA helixes.

The effect of the lipoplex structure has been proved to be important in the early stage of the transfection.[5,67,68] Nowadays, it is assumed that the main entry trail to the cells is the endocytosis, being the cationic lipoplex captured by an anionic endosomal vesicle formed from the cellular membrane.[11] It has also been confirmed[5,67] that the interaction between positive charged lipoplexes and anionic membranes is strongly dependent on the lipoplex structure, lamellar or hexagonal, even when both structures contain a zwitterionic lipid, as DOPE. In fact, lipoplexes with lamellar structure captured by endosomal vesicles remain stable, with no fusion occurring between the lipoplex and the vesicle being the DNA release relatively low. On the contrary, lipoplexes with hexagonal structure rapidly fused with the anionic endosomal vesicle, which provokes a loosing of the lipoplex condensed structure. Accordingly, the inverted lipoplex hexagonal structure inside endosome favors,

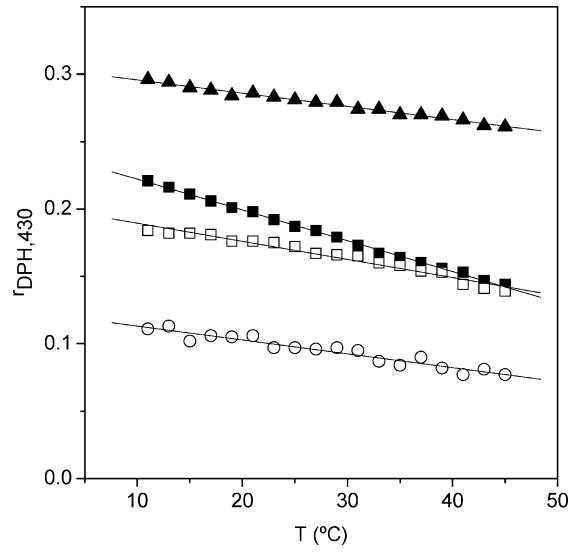

Figure 7. Fluorescence anisotropy at 430 nm ($r_{DPH,430}$) of DPH as a function of temperature for (i) DC-Chol/DOPE liposomes with α = 1 (solid triangles) and α = 0.5 (solid squares) and (ii) DC-Chol/DOPE/DNA lipoplexes at $L/D = 7$, with α = 0.5 (open squares) and α = 0.3 (open circles). Errors by light scattering are less than 3%. DPH (included in liposome membranes by following a procedure widely explained elsewhere[58]) was excited at 360 nm and its fluorescence emission was recorded at 430 nm, with slit widths of 2.5 nm for both the excitation and the emission.

after fusion, that DNA is easier released and expelled to the cytoplasm.[67] For that reason, research groups involved in this subject are looking for hexagonal or cubic lipoplex structures with proven better efficiency in transfection than lamellar ones.[68,69] In this respect, it can be concluded that the lipoplex studied in this work, DC-Chol/DOPE-DNA, is potentially an adequate gene transfector if the liposome composition presents a deficit on the cationic component, because an inverted hexagonal phase has been found in such cases.

It is known that fluorescence anisotropy, *r*, serves as a measurement of membrane fluidity, since, as long as membrane becomes more fluid, the degree of rotation of an excited fluorophore placed within will increase, and, accordingly, anisotropy decreases. Figure 7 shows anisotropy values of the non polar DPH fluorophore buried within the hydrophobic part of the lipidic bilayer of DC-Chol/DOPE liposomes, in the absence and in the presence of DNA, as a function of temperature. It can be noticed that the fluidity of the liposome bilayer increases (anisotropy monotonously decreases) with increasing temperature in both cases. In fact, it has been previously reported[59] that the presence of DOPE as helper lipid induces a rather monotonous decrease on anisotropy. Given that no change on the slope of *r* versus *T* profiles in Figure 7 is observed, it can be concluded that gel-to-fluid transition temperatures, T_m, of pure DC-Chol and mixed DC-Chol/DOPE liposomes are below the experimental temperature range studied, which confirms that liposome and lipoplexes bilayers are in the fluid state at physiological temperature, and, accordingly, at the temperature of both the electrochemical and SAXS experiments carried on in this work. Other interesting conclusions can be also extracted from Figure 7: (*i*) The presence of DOPE as helper lipid favors the fluidity of the liposome (decreases *r* at any *T*), as previously found for other lipoplexes.[34,39,41,42,44,45,48,50,51,59] It is well-known that the inclusion of DOPE, increases liposome stability, due in part to its low T_m, reducing T_m of the mixture below room temperature, and also to its structure, a typical cone-shaped molecule (with a packing parameter above 1) with a

known tendency to form inverted hexagonal phases.[65,67] (*ii*) For a fixed liposome composition, α, the interaction with DNA does not modify the anisotropy versus *T* profiles and does not seem to affect very much the fluidity of the bilayer because anisotropy values for DC-Chol/DOPE-DNA lipoplexes are similar to those for the mixed liposome, with this feature being more evident as the temperature increases. Similar results have been reported for other lipoplexes,[59] while a decrease on lateral difussion of the lipids by DNA complexation has been found in surfoplexes (through anisotropy studies)[58] and lipoplexes (by NMR experiments).[70] (iii) However, the decrease of cationic lipid composition, α, provokes a clear decrease of around 30% on anisotropy values for the resulting lipoplexes. Lipofection efficiency is known to be quite influenced by bilayer fluidity of lipoplexes. At this respect, anisotropy measurements represent a very helpful tool to predict the potential efficacy of transfection process. Anisotropy levels of less than 0.2−0.3 are believed to be related with enough fluid structures to allow for a potentially efficient transfection process.[50] It means that a low content of cationic lipid on the mixed liposomes, with the zwitterionic lipid being the major component, makes the resulting lipoplex more fluid, and, consequently, potentially more efficient on transfecting DNA to the cell. This last conclusion is consistent with that one extracted from SAXS results, that show the presence of hexagonal phases at low α values, and points again to the low contents on cationic lipid as a potentially favoring factor on transfection.

Conclusions

A series of experimental techniques (electrophoretic mobility, SAXS, and fluorescence anisotropy), together with a theoretical aggregation−disaggregation model, has evidenced that DC-Chol/DOPE cationic liposomes, with an average hydrodynamic diameter of (120 ± 10) nm, properly condense and compact CT-DNA, the liposome and lipoplex compositions being key factors on the properties and structure of the resulting lipoplex. The electrochemical experiments revealed that lipoplex formation process is characterized by a strong entropically driven surface electrostatic interaction. The isoneutrality of the lipoplex thus formed, determined by zeta potential and calculated with the model, decreases with the content of cationic lipid on the mixed liposome. Phase diagrams, theoretically calculated, show a clear effect of the liposome composition: as long as the molar fraction of cationic lipid decreases, the boundary concentration lines ($S_a(P)$ for aggregation of lipoplexes, $S_\phi(P)$ for isoneutrality, and $S_d(P)$ for disaggregation of clusters, are separated from each other (liposome concentration range gets wider) and their slopes decrease. It means that those lipoplexes consisting of liposomes with the cationic lipid as the major component require a lower number of liposomes to induce charge inversion. Furthermore, theoretical predictions point again to DOPE as a very adequate helper lipid and to DC-Chol as a promising cationic lipid, with improved characteristics compared to those of the dialkylamines and diols families. SAXS patterns have revealed that, irrespectively of the lipoplex charge ratio, DC-Chol/DOPE-DNA lipoplexes show an inverted micellar hexagonal structure, H_{II}, usually related with improved cell transfection efficiency, when the cationic lipid composition on the mixed liposomes, α, is 0.2, while for higher contents the lipoplexes show a lamellar structure, L_α. The latest structure is characterized by (i) a periodic distance, *d*, that remains roughly constant at 6.8 ± 0.2 nm on average, irrespective of liposomes and lipoplex (*L*/*D* and CR) compositions; (ii) the thickness of the DNA monolayer, d_w, of around 2.8 ± 0.2 nm (with $d_m \approx 4.0$ nm) is independent of α, *L*/*D*, and CR and very consistent with the presence of a monolayer of hydrated DNA helixes; and (iii) the separation between the DNA helixes in the aqueous monolayer, d_{DNA}, which remains approximately constant with α and *L*/*D*, falls within an average value of 5.2 ± 0.2 nm. On the other hand, the H_{II} structure is characterized by (i) the spacing of the cell unit, *a*, that remains almost constant with CR at around 6.7 ± 0.2 nm, indicating that, in the hexagonal structure, DNA helixes are more separated than in the lamellar one and (ii) the diameter inside the inverted micelle cylinder (equivalent to d_w in the lamellar structure), with a value of 2.7 ± 0.2 nm, is also consistent with the presence of DNA helixes. Fluorescence anisotropy results have revealed that low cationic lipid contents on the mixed liposome tends to favor more fluid bilayers, which in turn is a potential advantage on transfecting cells. Considering the whole information given by both the experiments and the calculus reported in this work, it can be concluded that DC-Chol/DOPE mixed liposomes are potentially adequate DNA vectors on gene therapy, mostly when they consist of a low content on the cationic lipid, although tranfection assays would be necessary to unequivocally ensure it.

Acknowledgment. The authors thank MICINN of Spain (Projects Nos. CTQ2009-10002BQU and UCMA05-33-010) and to the Comunidad Autónoma of Madrid (Project No. S-SAL-0249-2006). A.N. thanks MICINN of Spain (Project No. MAT2008-03232) and CSIC (Project No. PIE200750-I021). A.M.-M. thanks the Ministerio de Ciencia e Innovación (Project MAT2009-13155-C04-04) and Junta de Andalucía (Projects P07-FQM-02517 and P09-FQM-4698). Authors also thank C. Aicart for carrying on gel agarose electrophoresis experiments at the Biochemistry and Molecular Biology Department of the UCM of Spain.

References and Notes

(1) Felgner, J. H.; Gadek, T. R.; Holm, M.; Roman, R.; Chan, H. W.; Wenz, M.; Northrop, J. P.; Ringold, G. M.; Danielsen, M. *Proc. Natl. Acad. Sci. U.S.A.* **1987**, *84*, 7413–7417.
(2) Felgner, P. L.; Heller, M. J.; Lehn, J. M.; Behr, J.-P.; Szoka, F. C. *Artificial Self-Assembling Systems for Gene Delivery*; American Chemical Society: Washington, DC, 1996.
(3) Mahato, R. I.; Kim, S. W. *Pharmaceutical Perspectives of Nucleic Acid-Base Therapeutics*; Taylor and Francis: London, 2002.
(4) Lasic, D. D. *Liposomes in Gene Delivery*; CRC Press: Boca Raton, FL, 1997.
(5) Ewert, K.; Slack, N. L.; Ahmad, A.; Evans, H. M.; Lin, A. J.; Samuel, C. E.; Safinya, C. R. *Curr. Med. Chem.* **2004**, *11*, 133–149.
(6) Lonez, C.; Vandenbranden, M.; Ruysschaert, J. M. *Prog. Lipid Res.* **2008**, *47*, 340–347.
(7) Ma, B. C.; Zhang, S. B.; Jiang, H. M.; Zhao, B. D.; Lv, H. T. *J. Controlled Release* **2007**, *123*, 184–194.
(8) Safinya, C. R.; Ewert, K.; Ahmad, A.; Evans, H. M.; Raviv, U.; Needleman, D. J.; Lin, A. J.; Slack, N. L.; George, C.; Samuel, C. E. *Philos. Trans. R. Soc., A* **2006**, *364*, 2573–2596.
(9) Dias, R. S.; Lindman, B. *DNA Interaction with Polymers and Surfactants*; Wiley and Sons: Hoboken, NJ, 2008.
(10) Ahmad, A.; Evans, H. M.; Ewert, K.; George, C. X.; Samuel, C. E.; Safinya, C. R. *J. Gene Med.* **2005**, *7*, 739–748.
(11) Lin, A. J.; Slack, N. L.; Ahmad, A.; George, C. X.; Samuel, C. E.; Safinya, C. R. *Biophys. J.* **2003**, *84*, 3307–3316.
(12) Esposito, C.; Generosi, J.; Mossa, G.; Masotti, A.; Castellano, A. C. *Colloids Surf., B* **2006**, *53*, 187–192.
(13) Choi, J. S.; Lee, E. J.; Jang, H. S.; Park, J. S. *Bioconjugate Chem.* **2001**, *12*, 108–113.
(14) Farhood, H.; Serbina, N.; Huang, L. *Biochim. Biophys. Acta* **1995**, *1235*, 289–295.
(15) Kreiss, P.; Cameron, B.; Rangara, R.; Mailhe, P.; Aguerre-Charriol, O.; Airiau, M.; Scherman, D.; Crouzet, J.; Pitard, B. *Nucleic Acid Res.* **1999**, *27*, 3792–3798.

(16) Caplen, N. J.; Alton, E. W.; Middleton, P. G.; Dorin, J. R.; Stevenson, B. J.; Gao, X.; Durham, S. R.; Jeffrey, P. K.; Hodson, M. E. *Nat. Med.* **1995**, *1*, 39–46.
(17) Bajaj, A.; Kondiah, P.; Bhattacharya, S. *J. Med. Chem.* **2007**, *50*, 2432–2442.
(18) Bajaj, A.; Kondaiah, P.; Bhattacharya, S. *Bioconjugate Chem.* **2007**, *18*, 1537–1546.
(19) Ding, W.; Hattori, Y.; Higashiyarna, K.; Maitani, Y. *Int. J. Pharm.* **2008**, *354*, 196–203.
(20) Ghosh, Y. K.; Visweswariah, S. S.; Bhattacharya, S. *Bioconjugate Chem.* **2002**, *13*, 378–384.
(21) Reynier, P.; Briane, D.; Coudert, R.; Fadda, G.; Bouchemal, N.; Bissieres, P.; Taillandier, E.; Cao, A. *J. Drug Targeting* **2004**, *12*, 25–38.
(22) Zuidam, N. J.; Barenholz, Y. *Biochim. Biophys. Acta* **1998**, *1368*, 115–128.
(23) Caracciolo, G.; Caminiti, R. *Chem. Phys. Lett.* **2005**, *411*, 327–332.
(24) Caracciolo, G.; Pozzi, D.; Amenitsch, H.; Caminiti, R. *Langmuir* **2005**, *21*, 11582–11587.
(25) Ciani, L.; Casini, A.; Gabbiani, C.; Ristori, S.; Messori, L.; Martini, G. *Biophys. Chem.* **2007**, *127*, 213–220.
(26) Sternberg, B.; Sorgi, F. L.; Huang, L. *FEBS Lett.* **1994**, *356*, 361–366.
(27) Congiu, A.; Pozzi, D.; Esposito, C.; Castellano, C.; Mossa, G. *Colloids Surf., B* **2004**, *36*, 43–48.
(28) Rodriguez-Pulido, A.; Ortega, F.; Llorca, O.; Aicart, E.; Junquera, E. *J. Phys. Chem. B* **2008**, *112*, 12555–12565.
(29) Lasic, D. D.; H., S.; Stuart, M. A. C.; R., P.; Frederik, P. *J. Am. Chem. Soc.* **1997**, *119*, 832–833.
(30) Barreleiro, P. C. A.; Olofsson, G.; Brown, W.; Edwards, K.; Bonassi, N. M.; Feitosa, E. *Langmuir* **2002**, *18*, 1024–1029.
(31) Feitosa, E.; Alves, F. R.; Niemiec, A.; Oliveira, M.; Castanheira, E. M. S.; Baptista, A. L. F. *Langmuir* **2006**, *22*, 3579–3585.
(32) Salvati, A.; Ciani, L.; Ristori, S.; Martini, G.; Masi, A.; Arcangeli, A. *Biophys. Chem.* **2006**, *121*, 21–29.
(33) Gustafsson, J.; Arvidson, G.; Karlsson, G.; Almgren, M. *Biochim. Biophys. Acta* **1995**, *1235*, 305–312.
(34) Xu, Y. H.; Hui, S. W.; Frederik, P.; Szoka, F. C. *Biophys. J.* **1999**, *77*, 341–353.
(35) Hirsch-Lerner, D.; Zhang, M.; Eliyahu, H.; Ferrari, M. E.; Wheeler, C. J.; Barenholz, Y. *Biochim. Biophys. Acta* **2005**, *1714*, 71–84.
(36) Janoff, A. S. *Liposomes: Rational Design*; Marcel Dekker: New York, 1999.
(37) Rosoff, M. *Vesicles*; Marcel Dekker: New York, 1996.
(38) Rädler, J. O.; Koltover, I.; Jamieson, A.; Salditt, T.; Safinya, C. R. *Langmuir* **1998**, *14*, 4272–4283.
(39) Birchall, J. C.; Kellaway, I. W.; Mills, S. N. *Int. J. Pharm.* **1999**, *183*, 195–207.
(40) Lobo, B. C.; Rogers, S. A.; Choosakoonkriang, S.; Smith, J. G.; Koe, G. S.; Middaugh, C. R. *J. Pharm. Sci.* **2001**, *91*, 454–466.
(41) Eastman, S. J.; Siegel, C.; Tousignant, J.; Smith, A. E.; Cheng, S. H.; Scheule, R. K. *Biochim. Biophys. Acta* **1997**, *1325*, 41–62.
(42) Lakowicz, J. R. *Principles of Fluorescence Spectroscopy*; Kluwer Acad./Plenum: New York, 1999.
(43) MacDonald, R. C.; Ashley, G. W.; Shida, M. M.; Rakhmanova, V. A.; Tarahovsky, Y. S.; Pantazatos, D. P.; Kennedy, M. T.; Pozharski, E. V.; Baker, K. A.; Jones, R. D.; Rosenzweig, H. S.; Choi, K. L.; Qiu, R.; McIntosh, T. J. *Biophys. J.* **1999**, *77*, 2612–2629.
(44) Tarahovsky, Y. S.; Koynova, R.; MacDonald, R. C. *Biophys. J.* **2004**, *87*, 1054–1064.
(45) Bhattacharya, S.; Mandal, S. S. *Biochemistry* **1998**, *37*, 7764–7777.
(46) Geall, A. J.; Eaton, M. A. W.; Baker, T.; Catterall, C.; Blagbrough, I. S. *FEBS Lett.* **1999**, *459*, 337–342.
(47) Borenstain, V.; Barenholz, Y. *Chem. Phys. Lipids* **1993**, *64*, 117–127.
(48) Hirsch-Lerner, D.; Barenholz, Y. *Biochim. Biophys. Acta* **1998**, *1370*, 17–30.
(49) Lentz, B. R.; Moore, B. M.; Barrow, D. A. *Biophys. J.* **1979**, *25*, 489–494.
(50) Regelin, A. E.; Fankhaenel, S.; Gurtesch, L.; Prinz, C.; von Kiedrowski, G.; Massing, U. *Biochim. Biophys. Acta* **2000**, *1464*, 151–164.
(51) Ryhänen, S. J.; Säily, M. J.; Paukku, T.; Borocci, S.; Mancini, G.; Holopainen, J. M.; Kinnunen, P. K. *Biophys. J.* **2003**, *84*, 578–587.
(52) Sennato, S.; Bordi, F.; Cametti, C. *J. Chem. Phys.* **2004**, *121*, 4936–4940.
(53) Sennato, S.; Bordi, F.; Cametti, C.; Di Biasio, A.; Diociaiuti, A. *Colloids Surf., A* **2005**, *270−271*, 138–147.
(54) Rodriguez-Pulido, A.; Aicart, E.; Llorca, O.; Junquera, E. *J. Phys. Chem. B* **2008**, *112*, 2187–2197.
(55) Barreleiro, P. C. A.; Lindman, B. *J. Phys. Chem. B* **2003**, *107*, 6208–6213.
(56) Mel'nikov, S. M.; Lindman, B. *Langmuir* **1999**, *15*, 1923–1928.
(57) Gonçalves, E.; Debs, R. J.; Heath, T. D. *Biophys. J.* **2004**, *86*, 1554–1563.
(58) Rodriguez-Pulido, A.; Aicart, E.; Junquera, E. *Langmuir* **2009**, *25*, 4402–4411.
(59) Rodriguez-Pulido, A.; Martin-Molina, A.; Rodriguez-Beas, C.; Llorca, O.; Aicart, E.; Junquera, E. *J. Phys. Chem. B* **2009**, *113*, 15648–15661.
(60) Nguyen, T. T.; Shklovskii, B. I. *J. Chem. Phys.* **2001**, *114*, 5905–5916.
(61) Nguyen, T. T.; Shklovskii, B. I. *J. Chem. Phys.* **2001**, *115*, 7298–7308.
(62) Hunter, R. J. *Foundations of Colloid Science*; Oxford Science: Oxford, 1995.
(63) de Lima, M. C. P.; Simoes, S.; Pires, P.; Faneca, H.; Duzgunes, N. *Adv. Drug Delivery Rev.* **2001**, *47*, 277–294.
(64) Hui, S. W.; Langner, M.; Zhao, Y.-L.; Ross, P.; Hurley, E.; Chan, K. *Biophys. J.* **1996**, *71*, 590–599.
(65) Rädler, J. O.; Koltover, I.; Salditt, T.; Safinya, C. R. *Science* **1997**, *275*, 810–814.
(66) Koltover, I.; Salditt, T.; Safinya, C. R. *Biophys. J.* **1999**, *77*, 915–924.
(67) Koltover, I.; Salditt, T.; Rädler, J. O.; Safinya, C. R. *Science* **1998**, *281*, 78–81.
(68) Pozzi, D.; Caracciolo, G.; Caminiti, R.; De Sanctis, S. C.; Amenitsch, H.; Marchini, C.; Montani, M.; Amici, A. *ACS Appl. Mater. Interfaces* **2009**, *1*, 2237–2249.
(69) Bouxsein, N. F.; McAllister, C. S.; Ewert, K. K.; Samuel, C. E.; Safinya, C. R. *Biochemistry* **2007**, *46*, 4785–4792.
(70) Leal, C.; Sandstrom, D.; Nevsten, P.; Topgaard, D. *Biochim. Biophys. Acta* **2008**, *1778*, 214–228.

BM1008124